Progress In Electromagnetics Research, PIER 85, 289–302, 2008

MICROWAVE IMAGING A BURIED OBJECT BY THE GA AND USING THE S_{11} PARAMETER

F. Li, X. Chen, and K. Huang

College of Electronics and Information Engineering
Sichuan University
Chengdu 610064, P. R. China

Abstract—This paper explores the feasibility of microwave imaging a buried object by the GA and using the S_{11} parameter of a radiation antenna rather than data of the scattered electromagnetic field. To improve the efficiency of the GA-based algorithm, a technique of limiting the location of the buried object prior to the implement of the GA is proposed, and the GA is parallelized and executed on a PC cluster. A few numerical examples are presented, in which the dimension and location of a 3-D object buried in the earth are recovered. Results validate the proposed GA-based microwave imaging algorithm.

1. INTRODUCTION

Microwave imaging a buried object is a class of electromagnetic inverse problems. It has been widely used in sensing and remote-sensing applications, such as geophysical exploration, medical imaging, nondestructive evaluation, and etc [1]. Many imaging methods have been proposed, e.g., the Genetic Algorithm (GA) [1], the diffraction tomographic (DT) algorithm [2], the Born iterative method (BIM), the distorted Born iterative method (DBIM) [3, 4], the memetic algorithm [5], and etc [6–8].

The GA is an admirable global optimization algorithm that uses the genetic operators (selection, crossover, mutation) to search through a coding of a parameter space. It does not depend on initial set of conditions, and is able to converge to the global extreme of the problem [9]. Hence the GA has been widely employed in microwave imaging problems [1, 9–14].

There are some problems exist in the previous works on the GA-based microwave imaging. Firstly, most works are based on

the utilization of the data of scattered electromagnetic field, but in practical cases, the measurement of the scattered electromagnetic field is very inconvenient. Especially many works even require data of the scattered field at many points [1–14] or at more than one frequency [15–17], which makes a big trouble for practically applications of the microwave imaging technology. Secondly, in previous works [1–17], measurement points are essentially considered as sizeless points, and the dimension of antennas or probers are ignored, which may brings forth big errors in those cases; Thirdly, to reduce the complexity and consumed time of the imaging computation, the imaging domains in most works are very small, typically only a few wavelengths, which is not necessarily true in many practical cases.

This paper investigates the microwave imaging based on the GA for determining the location and dimension of a three-dimensional (3-D) object buried in a large-dimension and lossy earth. To overcome the problems mentioned above, it for the first time explores the feasibility of microwave imaging using the S_{11} parameter (input return loss) of a radiation antenna rather than the data of the scattered electromagnetic field by the buried object. In comparison with the data of the scattered field, the S_{11} parameter can be easily and quickly measured by employing a network analyzer.

The GA is a time-consuming algorithm [18, 19]. To improve its efficiency and reduce its computation time, a new technique of limiting the location of a buried object prior to the implement of the GA is proposed, and the GA is parallelized and run on a PC cluster.

In the following, the second section devotes to illustrate the imaging configuration. The proposed microwave imaging algorithm is introduced in the third section. A few numerical examples and their results are presented in the fourth section.

2. IMAGING CONFIGURATION

As illustrated in Fig. 1, in this work, an object with electromagnetic parameters ε_s, $\mu_s = \mu_0$, and σ_s is buried in the earth. The air is assumed to be $\varepsilon_a = \varepsilon_0$, $\mu_a = \mu_0$, and $\sigma_a = 0$. The earth is assumed to be homogenous and lossy with $\varepsilon_e = 2\varepsilon_0$, $\mu_e = \mu_0$, and $\sigma_e = 0.001\,\mathrm{s/m}$.

A bowtie antenna with wideband properties is employed as a radiation antenna. Its configuration is shown in Fig. 2. The antenna is placed 10 mm above the earth, and radiates microwave power covering a frequency band from 0.5 GHz to 2 GHz. At 1000 frequency points evenly distributed in the frequency band, the S_{11} parameter of the antenna is measured by using a network analyzer during microwave imaging procedures.

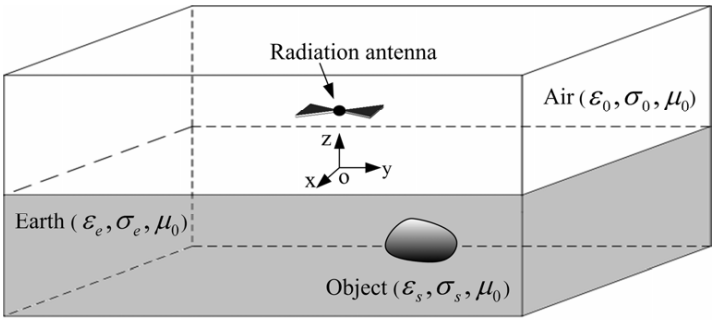

Figure 1. Microwave imaging configuration.

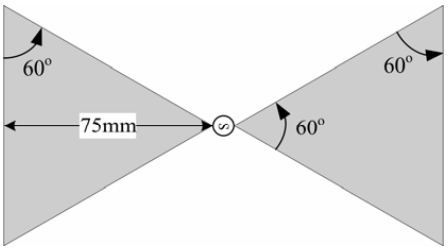

Figure 2. The bowtie antenna as a radiation antenna in the microwave imaging procedure.

The whole microwave imaging domain is about $100\lambda \times 100\lambda \times 1\lambda$, where λ is the wavelength at the frequency of 1 GHz. A coordinate system is set up, in which the planar interface separating the air and the earth is located at $z = 0$ and the z axis passes through the center point of the bowtie antenna. All dimensions in the coordinate system are in millimeter, so the bowtie antenna is located at (0, 0, 10 mm).

In this work, the location and dimension of the buried object are unknowns and need to be recovered by a microwave imaging procedure.

3. THE MICROWAVE IMAGING ALGORITHM

3.1. The S_{11} Parameter of the Radiation Antenna

To estimate the impact of a buried object to the S_{11} parameter of the bowtie antenna, a metal sphere with a radius of 30 mm is assumed to be embedded in the earth. By making use of the FDTD (Finite-Difference Time-Domain) method, corresponding S_{11} parameters of the bowtie antenna under different conditions are computed and illustrated in

Fig. 3. From the figure, one can observe that the existence of a buried object and its location have an obvious impact on the S_{11} parameter of the antenna. Therefore the S_{11} parameter can be utilized in the microwave imaging for recovering physical information of a buried object.

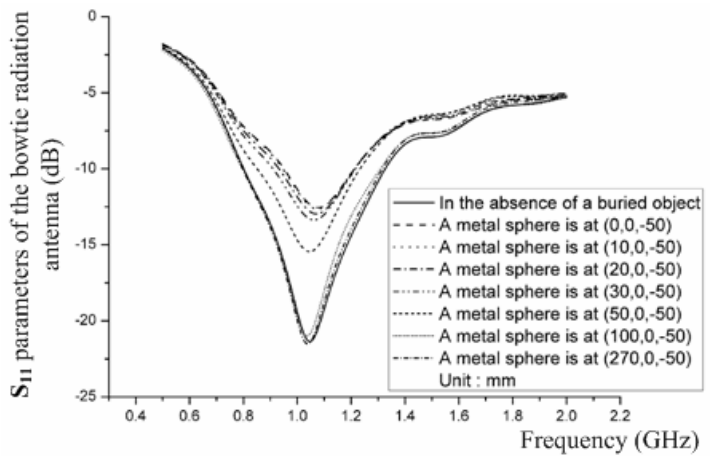

Figure 3. S_{11} parameters of the bowtie radiation antenna under various conditions.

In this figure, the location of the metal sphere is denoted by the coordinate values of its center point.

3.2. The Forward Computation

The FDTD [20] method is efficient for modeling 3-D inhomogeneous objects and complex geometries. Hence in this work, a three-dimensional FDTD code is wrote to compute S_{11} parameters of the bowtie antenna under various conditions, which are needed for the GA-based microwave imaging. The computational region is discretized by Yee's grids [21, 22], and a perfectly matched layer (PML) absorbing boundary condition (ABC) [22–25] is used to truncate the computational region.

3.3. The GA-Based Microwave Imaging

The Genetic Algorithm (GA) [9–12] is a robust, stochastic and global optimization method modeled on the principles and concepts of natural selection and evolution. The basic ideal of its applications in the microwave imaging is recasting a microwave imaging problem from an

inverse scattering problem to a global optimization problem. It uses an iterative procedure that starts with a randomly selected population of potential solutions, and then gradually evolves toward a better solution through the application of the genetic operators, i.e., reproduction, crossover, and mutation operators. All unknown parameters, e.g., location and dimension of a buried object in this work, are coded by the following equation to a serial of binary codes:

$$p = p_{\min} + \frac{p_{\max} - p_{\min}}{2^L - 1} \sum_{i=0}^{L-1} b_i 2^i \tag{1}$$

where p is a unknown parameter, $p_{\min}$ and $p_{\max}$ are the minimum and maximum values admissible for p, b_i is the L-bit string of the binary representation of p. Here, $p_{\min}$ and $p_{\max}$ are usually determined by prior knowledge of the object.

The GA starts with a set of randomly constituted trial solutions that is called individuals. In this research, an individual is a set of location and dimensional parameters of a trial buried object. A collection of the individuals forms a population. Then, for every trial buried object, the FDTD method is employed to compute the S_{11} parameter of the radiation antenna. Such calculated S_{11} parameter is compared with the measured S_{11} parameter. The difference between these two sets of S_{11} parameters indicates how close the location and dimensional parameters of a trial object are to those of the actual buried object. By defining a fitness function, the difference between the measured and calculated S_{11} parameters can be expressed by a fitness value. Assuming the S_{11} parameters of the radiation antenna are measured or calculated in a frequency band from f_L to f_H, in this work, the fitness function is defined as,

$$Fitness = 1 - \sqrt{\frac{\sum_{f=f_L}^{f_H} \left(S_{11}^{measured}(f) - S_{11}^{calculated}(f) \right)^2}{\sum_{f=f_L}^{f_H} \left(S_{11}^{measured}(f) \right)^2}} \tag{2}$$

where $Fitness$ is the fitness value, $S_{11}^{measured}$ and $S_{11}^{calculated}$ are the measured and calculated S_{11} parameters of the radiation antenna respectively.

One observes from the Equation (2) that when the S_{11} difference goes to zero, the fitness value would approach to one. Thus, the inverse problem of the microwave imaging is converted to a global

optimization, and the goal of the GA is to maximize the fitness value using the selection, crossover, and mutation operations through an iterative procedure, i.e., find out a trial buried object that would result in a fitness value close to 1.

3.4. The Parallel Computation

The GA-based microwave imaging usually invokes hundreds or even thousands forward FDTD computations, hence is computationally intensive. Since the GA exhibits an intrinsic parallelism and allows a very straightforward implementation on parallel computers, we implement the GA-based microwave imaging into parallel computation to make the computation more effective. The computation is parallelized in a master-slave model and is carried out in a Beowulf cluster system [1, 26, 27], which is composed of 32 processors interconnected by a fast 1000 Mb/s Ethernet and uses the message passing interface (MPI) library.

3.5. A Technique to Limit the Location of the Buried Object Prior to the Implement of the GA

Due to the large imaging domain in this work, the consumed time of directly implementing the GA into a microwave imaging may be unaffordable. Hence a technique, which is able to limit the location of the buried object prior to the implement of the GA, is presented.

It is obvious that the impact of the buried object on the S_{11} parameter of the radiation antenna is in inverse proportion to the distance between the radiation antenna and the buried object. We can measure and record the S_{11} parameter of the radiation antenna in the absence of a buried object. Here we denote the S_{11} parameter measured in the absence of a buried object as S'_{11}. If the buried object is far from the radiation antenna, the discrepancy between the measured S_{11} and S'_{11} should be quite small. Hence, in a microwave imaging procedure, the discrepancy between the measured S_{11} and S'_{11} can help us to judge whether the buried object is in the vicinity of the radiation antenna.

The discrepancy between the measured S_{11} parameter and S'_{11} is defined as,

$$DS_{11} = \sum_{f=F_L}^{f_H} \left(S_{11}(f) - S'_{11}(f)\right)^2 \tag{3}$$

The Table 1 lists the distance between the buried object and the radiation antenna, as well as the corresponding values of DS_{11}. From the table, we can observe that the value of DS_{11} is in the inverse

proportion to the distance. So the value of DS_{11} can help us to limit the location of the buried object.

Table 1. The values of DS_{11} vs the distance between the buried object and the radiation antenna. The radiation antenna is located at (0, 0, 10 mm).

Location of the buried object			Distance (mm)	DS_{11}
X (mm)	Y (mm)	Z (mm)		
0	10	−25	26.93	6.427355
0	20	−40	44.72	2.824615
0	0	−50	60.00	2.484087
30	0	−50	67.08	2.002562
100	0	−50	116.6	0.106043
270	0	−50	276.5	0.044081
300	300	−100	435.9	0.000640

In this work, prior to the implement of the GA in a microwave imaging, the radiation antenna is moved through the surface of the earth in the imaging domain point-by-point. At each point, the S_{11} parameter of the radiation antenna is measured and then the corresponding DS_{11} is computed. Finally, a point with biggest DS_{11} is selected and the buried object should be in its vicinity. A circle is drawn with the point as it center. The radius of the circle is very important and should be carefully determined by experience or numerical calculations, because it should be a good tradeoff between ensuring the object to be included in the circle and making the dimension of the circle to be as small as possible. In this work, based on results of some numerical calculations, we set the radius to be 30 mm. The area circumvented by the circle will be the new imaging domain for the GA-based microwave imaging, and it is usually much smaller than the original domain, so that the performance of the GA-based microwave imaging can be greatly speeded up.

4. NUMERICAL RESULTS

To validate the proposed GA-based microwave imaging method, in this section, sample numerical results are presented and analyzed.

In the first example, the 3-D buried object is assumed to be a metal sphere with a radius $R = 30$ mm and buried at (60 mm, 50 mm, −50 mm).

Firstly, by using the technique of limiting the location of the buried object introduced in the last section, we measured the S_{11} parameter of the radiation antenna in the absence of the buried object, and then moved the bowtie antenna on the surface of the earth through the whole imaging domain, and found the point with biggest DS_{11} is at (67.5 mm, 46.875 mm). Hence a new imaging domain, roughly with x from 37.5 mm to 97.5 mm and y from 16.875 mm to 76.875 mm, is determined. Its size is only 0.0003% of that of the original domain.

The GA is employed for recovering the radius R and location of the metal sphere in the new imaging domain. In the example, the location of the metal sphere is represented by the coordinate values of its center point, i.e., x_0, y_0, z_0. We adopts a binary GA, which employs tournament selection with elitism, single-point crossover with probability $p_c = 0.5$, jump mutation with probability $p_m = 0.2$. In a GA run, the GA uses 50 individuals in a generation.

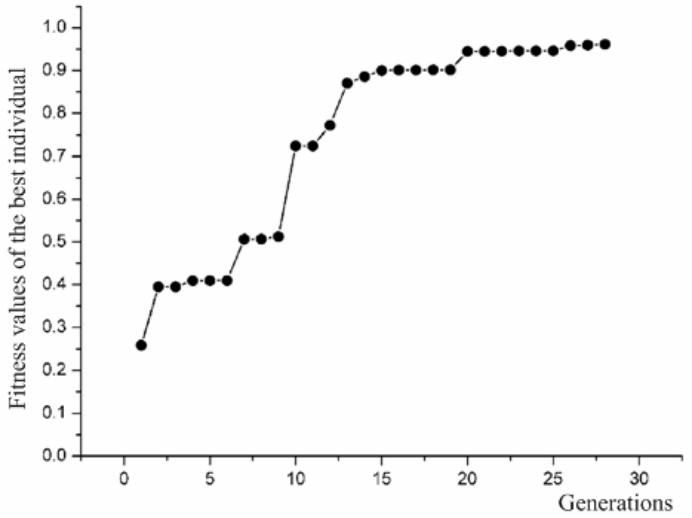

Figure 4. The fitness values of the best individual at different generations.

The fitness values, defined in Equation (3), for different generations are shown in Fig. 4. From this figure, one observes that the fitness values increases from generation to generation. At the 28th generation, it is optimized to 0.96153, which is very close to 1 and represents a satisfactory match between the "measured" and the "calculated" S_{11} parameters. Fig. 5 illustrates the microwave imaging results at the first and 28th generations as well as compares them with

the actual parameters of the buried sphere. From the figure, one can observe that results obtained by the GA at the first generation are quite different with the actual ones, but become very close to the actual ones at the 28th generation.

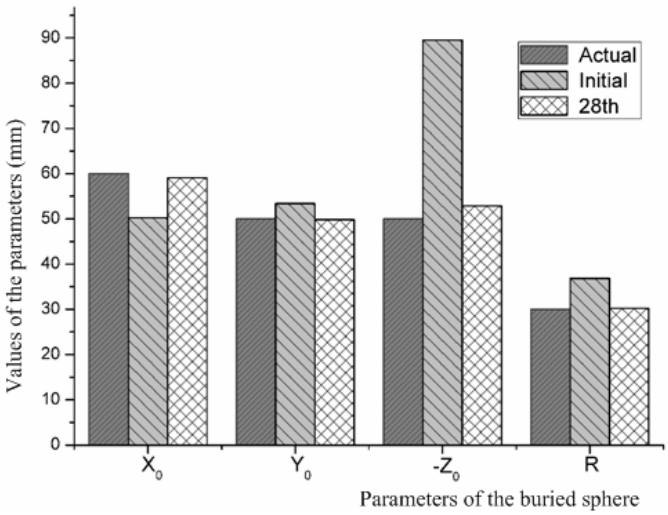

Figure 5. Parameters of the buried object obtained by the GA at the first and 28th generations as well as that of the actual object.

It should be pointed out that the parallel computation greatly reduced the computation time in this example. The imaging procedure consumes approximately 2 hours by using the cluster system with 32 processors, but if it is implemented on one processor, the consumed time is about 45 hours.

The second example is to estimate the sensitivity of the proposed algorithm to the noise. In this example, all "measurement" data, i.e., "measured" S_{11} parameters, are added 5% random noise. Except for the noisy "measurement" data, the imaging configuration and algorithm as well as parameters of the buried object and the GA are as the same as that in the previous example. Table 2 lists results obtained by the GA for different generations after introducing the noise. Though all "measurement" data have been added 5% random noise, and even the actual object has only a fitness value of 0.97328, the proposed algorithm still is able to precisely estimate the dimension and location of the buried metal sphere.

In the above two examples, the shape of the trial buried objects is assumed to be as the same as that of the actual buried object. In many practical cases, the shape of the buried object is complex or even can

not be known in advance, which may result in that the shape of the trial buried object adopted by the GA can not be selected as the same as that of the actual one. It is important to assess the effectiveness of the proposed microwave imaging algorithm in those cases.

Table 2. Results obtained by the GA for different generations after all "measurement" data are added 5% random noise.

Generation	X_0	Y_0	Z_0	R	Fitness Value
1	53.09587	59.18235	−55.95403	41.40604	0.2597063
10	50.26955	49.64135	−44.51786	29.88319	0.9163983
20	57.65259	49.63769	−50.14290	29.88319	0.9612671
28	57.65259	49.11033	−50.13741	29.88319	0.9806298
Actual Object	60	50	−50	30	0.9732800

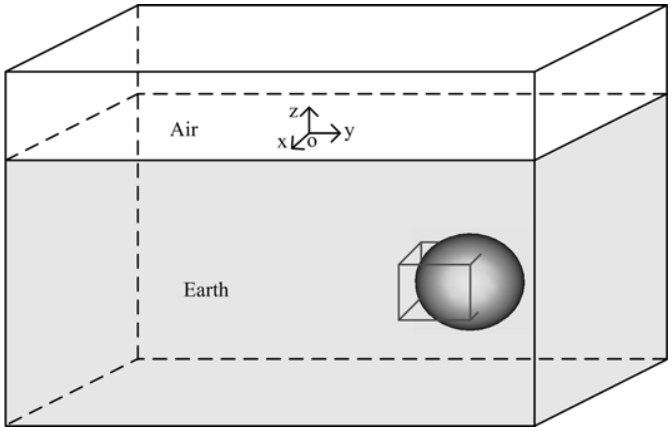

Figure 6. The image of the metal cube reconstructed by the GA at the 25th generation.

In this example, a metallic cube rather than a sphere is assumed to be buried at the (200 mm, −200 mm, −100 mm) with its length of 60 mm, but the trial object adopted by the GA is still a metallic sphere.

Figure 6 shows the image of the buried cube reconstructed by the GA at the 25th generation. For clearly demonstrating the reconstruction result, both the actual and the reconstructed object are displayed. We can observe that the location of the buried object is correctly recovered. The dimension of the buried object is retrieved

in a quite acceptable way, considering that the trial and actual buried objects are in different shapes.

5. CONCLUSION

In this paper, a GA-based algorithm has been proposed for microwave imaging an object buried in the earth. For reducing the difficulty of measurements in practical cases, it uses the S_{11} parameters of a radiation antenna rather than data of scattered electromagnetic field. To improve its efficiency, the proposed algorithm is parallelized and runs on a PC cluster as well as employs a technique of limiting the location of the buried object prior to the implement of the GA. Hence the proposed algorithm can be applied in microwave imaging cases with a large imaging domain.

Three numerical examples, in which the location and dimension of a 3-D metal object buried in the earth are recovered. Results validate the proposed GA-based microwave imaging algorithm.

ACKNOWLEDGMENT

This work was supported by a grant from the National High Technology Research and Development Program of China (863 Program, No. 2007AA01Z279).

REFERENCES

1. Chen, X., D. Liang, and K. Huang, "Microwave imaging 3-D buried objects using parallel genetic algorithm combined with FDTD technique," *Journal of Electromagnetic Waves and Applications*, Vol. 20, No. 13, 1761–1774, 2006.
2. Cui, T. J. and W. C. Chew, "Novel diffraction tomographic algorithm for imaging two-dimensional dielectric objects buried under a lossy earth," *IEEE Transactions on Geoscience and Remote Sensing*, Vol. 38, No. 4, 2033–2041, July 2000.
3. Cui, T. J., W. C. Chew, A. A. Aydiner, and S. Y. Chen, "Inverse scattering of two dimensional dielectric objects buried in a lossy earth using the distorted born iterative method," *IEEE Transactions on Geoscience and Remote Sensing*, Vol. 39, No. 2, 339–345, Feb. 2001.
4. Bucci, O. M., G. D'Elia, and M. Santojanni, "A fast multipole approach to 2D scattering evaluation based on a non redundant implementation of the method of auxiliary sources," *Journal of*

Electromagnetic Waves and Applications, Vol. 20, No. 13, 1715–1723, 2006.

5. Caorsi, S., A. Massa, M. Pastorino, M. Raffetto, and A. Randazzo, "Detection of buried inhomogeneous elliptic cylinders by a memetic algorithm," *IEEE Transactions on Antennas and Propagation*, Vol. 51, No. 10, 2878–2884, Oct. 2003.
6. Steinbauer, M. and R. Kubasek, "Numerical method of simulation of material influences in mr tomograohy," *Progress In Electromagnetics Research Letters*, Vol. 1, 205–210, 2008.
7. Zhong, X. M., C. Liao, W. Chen, Z. B. Yang, Y. Liao, and F. B. Meng, "Image reconstruction of arbitrary cross section conducting cylinder using UWB pulse," *Journal of Electromagnetic Waves and Applications*, Vol. 21, No. 1, 25–34, 2007.
8. Zacharopoulos, A., S. Arridge, O. Dorn, V. Kolehmainen, and J. Sikora, "3D shape reconstruction in optical tomography using spherical harmonics and BEM," *Journal of Electromagnetic Waves and Applications*, Vol. 20, No. 13, 1827–1836, 2006.
9. Chiu, C.-C. and W.-T. Chen, "Electromagnetic imaging for an imperfectly conducting cylinder by the genetic algorithm," *IEEE Transactions on Microwave Theory and Techniques*, Vol. 48, No. 11, Nov. 2000.
10. Caorsi, S. and M. Pastorino, "Two-dimensional microwave imaging approach based on a genetic algorithm," *IEEE Transactions on Antennas and Propagation*, Vol. 48, No. 3, March 2000.
11. Oka, S., H. Togo, N. Kukutsu, and T. Nagatsuma, "Latest trends in millimeter-wave imaging technology," *Progress In Electromagnetics Research Letters*, Vol. 1, 197–204, 2008.
12. Haupt, R. L., "An introduction to genetic algorithms for electromagnetics," *IEEE Antennas and Pmpagatiin Magazine*, Vol. 37, No. 2, April 1995.
13. Rostami, A. and A. Yazdanpanah-Goharrizi, "A new method for classification and identification of complex fiber Bragg grating using the genetic algorithm," *Progress In Electromagnetics Research*, PIER 75, 329–356, 2007.
14. Su, D. Y., D. M. Fu, and D. Yu, "Genetic algorithms and method of moments for the design of PIFAS," *Progress In Electromagnetics Research Letters*, Vol. 1, 9–18, 2008.
15. Kerr, Y. H., "The multi-frequency imaging microwave radiometer: applications to land surface parameter retrieval," *Geoscience and*

Remote Sensing Symposium, 1991. *IGARSS '91. 'Remote Sensing: Global Monitoring for Earth Management', International*.

16. Vertiy, A. and S. Gavrilov, "Imaging of buried object by tomography method using multifrequency regularization process," *11th Int. Conf. on Mathematical Methods in Electromagnetic Theory*, Kharkiv, Ukraine, June 26–29, 2006.
17. Guo, Y., S. A. Kassam, F. Ahmad, and M. Amin, "Reduced complexity multi-frequency imaging using active aperture synthesis," *IEEE Antenna and Propagation Society International Symposium*, 2004.
18. Li, C.-L., Y. Sun, L. Zhang, and X.-C. Wang, "A parallel micro-genetic algorithm its application," *Proceeding of the Fourth International Conference on Machine Learning and Cybernetics*, Guangzhou, August 18–21, 2005.
19. Meng, Z.-Q., "Autonomous genetic algorithm for functional optimization," *Progress In Electromagnetics Research*, PIER 72, 253–268, 2007.
20. Kunz, K. S. and R. J. Luebbers, *The Finite Difference Time Domain Method for Electromagnetics*, CRC Press, 1993.
21. Taflove, A., *Advance in Computational Electrodynamics*, Artech House, 1998.
22. Yee, K. S., "Numerical solution of initial boundary value problems involving Maxwell's equations in isotropic media," *IEEE Transactions on Antennas and Propagation*, Vol. 14, No. 4, 302–307, 1966.
23. Uduwawala, D., "Modeling and investigation of planar parabolic dipoles for GPR applications: A comparison with bow-tie using FDTD," *Journal of Electromagnetic Waves and Applications*, Vol. 20, No. 2, 53–56, 2006.
24. Ali, M. and S. Sanyal, "FDTD analysis of rectangular waveguide in receiving mode as ems sensors," *Progress In Electromagnetics Research B*, Vol. 2, 291–303, 2008.
    2008.
25. Ding, W., Y. Zhang, P. Y. Zhu, and C. H. Liang, "Study on electromagnetic problems involving combinations of arbitrarily oriented thin-wire antennas and inhomogeneous dielectric objects with a hybrid MoM-FDTD method," *Journal of Electromagnetic Waves and Applications*, Vol. 20, No. 11, 1519–1533, 2006.
26. Chen, X. and K. Huang, "Microwave imaging of buried inhomogeneous objects using parallel genetic algorithm combined with FDTD method," *Progress In Electromagnetics Research*,

PIER 53, 283–298, 2005.

27. Zhang, Y., X. W. Zhao, M. Chen, and C. H. Liang, "An efficient MPI virtual topology based parallel, iterative MoM-PO hybrid method on PC clusters," *Journal of Electromagnetic Waves and Applications*, Vol. 20, No. 5, 661–667, 2006.